INTERFACING METHODS FOR FLUIDICALLY-ASSEMBLED MICROCOMPONENTS

M. T. Tolley, A. Baisch, M. Krishnan, D. Erickson and H. Lipson
Mechanical and Aerospace Engineering, Cornell University, Ithaca, New York, USA

ABSTRACT

Here we present the design and implementation of electrical and mechanical interfaces for fluidically-assembled planar MEMS. We discuss the design and fabrication of systems of passive mechanical latches to bond microcomponents together and of electrical layers capable of establishing electrical connections with each other. We evaluate the ability of components with these interfaces to bond together within a microfluidic channel and to establish electrical circuits when assembled. This work supports the development of a novel microassembly strategy that bridges the gap between bottom-up self-assembly and top-down direct-manipulation technique. The ultimate goal of this research is the development of MEMS devices capable of the on-demand self-assembly, repair, and reconfiguration.

1. INTRODUCTION

Background

Self-assembly has shown promise as a practical alternative to pick-and-place assembly at the micro- and nanoscales [1,2]. Assembly techniques are necessary for the manufacture of increasingly complex micro/nanodevices with components with incompatible fabrication processes. As scales decrease, however, issues with adhesion, precision, device complexity, and assembly rates reduce the effectiveness of direct-manipulation techniques [3]. There has thus been a lot of interest in the design of components with interaction forces that cause them to assemble into useful structures.

At the microscale, self-assembly has been achieved using primarily surface energy minimization as the diving force with a medium such as solder or adhesive used to hold the assemblies together [4,5]. However, the ability of such techniques to assemble arbitrary structures is limited by the need to redesign the components for each new target structure. We have previously described an alternative directed fluidic assembly (DFA) method which allows the assembly of arbitrary structures from regular components while avoiding the limitations of direct-manipulation techniques [6]. Here we present the design and testing of mechanical and electrical interfaces for the microscale components assembled using our DFA method.

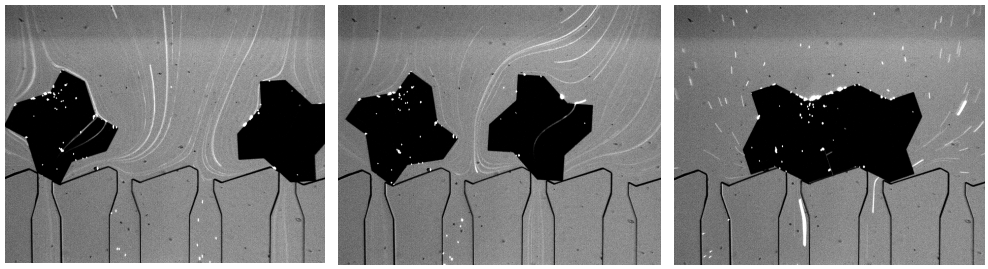
Directed fluidic assembly

The previously-described DFA concept is briefly summarized here: Regular components are introduced into a fluidic chamber, the walls of which are lined with a number of openings that connect to fluidic channels. The fluid flow through the chamber is controlled by regulating the fluid pressure in the channels. Hydrodynamic forces acting on the components cause them to move in response to the fluid flow. Thus the overall motion of the components is determined by the flow pattern which is controlled by valves on the fluidic channels.

Once the components come into contact with one-another or the chamber walls, local interaction forces take over to orient and align the components. This is caused by regular geometric patterns on the component sides and chamber walls.

In the experimental implementation of this concept, we restrict our components to two dimensions. Our components are 500μm by 500μm by 30μm tall silicon tiles and our fluidic chip is made of polydimethylsiloxane (PDMS) bonded to glass, fabricated using multilayer soft lithography [7]. Figure 1 is a demonstration of the assembly of two of these microtiles in a PDMS chamber.

The advances presented here relate to the mechanical and electrical interfacing of fluidically-assembled microtiles. We first discuss the design and testing of mechanical latches used to hold assemblies together. We then discuss the fabrication and testing of an electrical interface to allow the transfer of power and/or communication between tiles. These advances greatly expand the possibilities of DFA.



t = 53.32s *t = 55.91s* *t = 59.80s*

Figure 1: Frames taken from an optical microscope video of two 500μm x 500μm x 30μm microtiles being assembled in a PDMS microfluidic chamber by sequentially opening and closing outlet valves. Patterned sides and substrate cause the tiles to self-align when in contact. 3μm fluorescent particles visualize fluid's flow profile.

2. MECHANICAL INTERFACE

Design

Our goal was to design a planar passive latching mechanism to hold assembled tiles together. It was important that the force required to latch two tiles together was within the range of achievable hydrodynamic forces in our system. We thus used a model based on elementary beam mechanics to relate the latch design parameters to the force required to engage the latches.

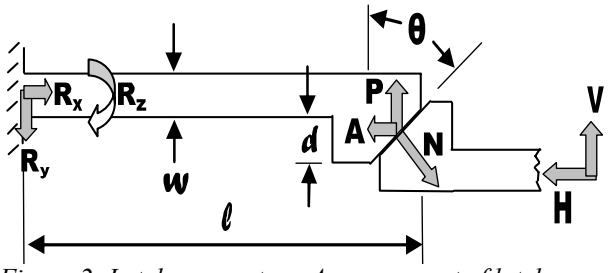


Figure 2: Latch parameters. A common set of latch parameters were chosen to compare various latch designs. The maximum required lateral force H on a contacting structure required to bend a latch it's full travel d was calculated for each design. l is the length of the latch, w is the width, t (in the z-direction) is the thickness, and θ is the angle of the latch head.

Figure 2 is a schematic of a latch with relevant design arameters and forces indicated. In our model we assume that the latch is a fixed, planar cantilever beam. We further assume that this beam is deflected by a complementary rigid shape which is constrained in the y-direction (due to pairing of opposing latches). This model also assumes no friction between the latch and complementary surfaces.

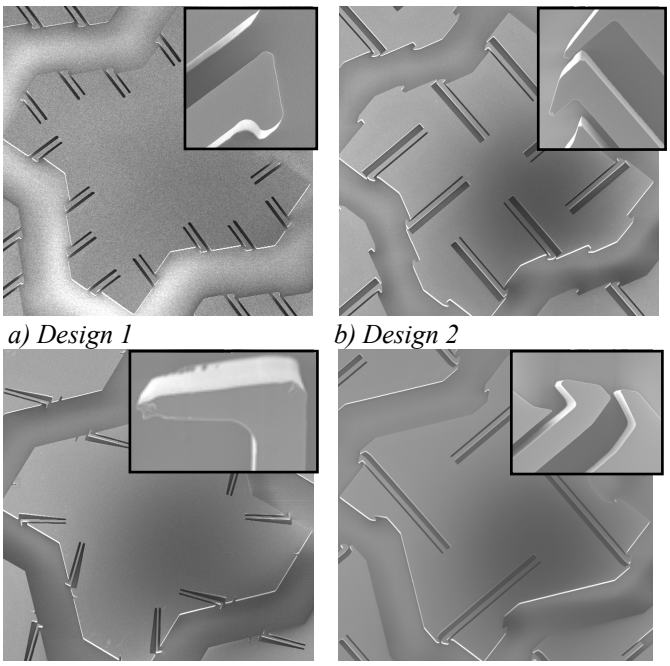
The perpendicular force P required to bend the cantilever tip by a deflection d is given by $P = 3dEI/l^3$ where E is the modulus of elasticity (we used 1.50×10^{11} Pa for silicon), I is the area moment of inertia of the beam's cross section, and l is the length of the beam. The area moment of inertia for a square beam is $I = w^3t/12$ where w is the width of the beam and t is its thickness. P can be related to the force N normal to the latch head by the trigonometric relationship $P = N\sin\theta$, similarly N is related to the horizontal force H by the relationship $H = N\cos\theta$. Finally, the total latching force F is this horizontal force multiplied by n, the total number of latches deflected per side $F = nH$. Putting this all together, the latching force in terms of the latch parameters is given by the equation:

$$F = \frac{ndw^3tE}{4l^3\tan\theta} \qquad (1)$$

Design	N	L (μm)	W (μm)	D (μm)	Bias (μm)	θ (°)	F (μN)
1	4	65.8	10.0	2.5	0.23	26.6	**62498**
2	4	158.0	10.0	5.0	0.31	34.0	**6527**
3	4	97.2	5.0	11.0	0.40	60.5	**2176**
4	2	279.7	10.0	10.0	0.58	39.8	**803**
5	2	280.3	5.0	6.0	0.45	49.4	**33**
6	2	280.3	3.0	6.0	0.45	49.4	**5**

Table 1: Latch design parameters

Various tile designs (Fig. 3) were created by varying the parameters in Equation (1) while the overall shape and size of the tiles were held constant. Table 1 summarizes the parameters chosen for each design. Note that the dimensions are the nominal design dimensions chosen so two tiles mate exactly. During fabrication the tile patterns were slightly overexposed in order to leave a clearance between the latching parts. These fabrication biases were measured from SEM images of the fabricated tiles and included in Table 1. The predicted latching force for each tile design was then calculated taking these biases into account.



a) Design 1 *b) Design 2*

c) Design 3 *d) Design 4*

Figure 3: Latching microtile designs. Scanning electron microscope images of latching 500μm square microtiles with latch detail insets. Designs 5 and 6 (not shown) are identical to Design 4 except with smaller latches.

Fabrication

Batches of the six microtile designs were each fabricated from a silicon-on-insulator (SOI) wafer with a 30 μm device layers and 1 μm thick buried oxide. A 7 μm layer of SPR 220 series photoresist was patterned on each wafer by contact alignment. The tile outlines were then etched through the device layer with a deep Bosch etch. The tiles were then released using a wet etch with 49% HF, and collected by filtration.

Results

The efficacies of the six tile designs in Figure 3 were tested experimentally. Designs 1 through 3 were found not to latch within the limit of attainable hydrodynamic forces in the microfluidic chamber. However, it was possible to latch these designs with direct manipulation (Fig. 4a). Design 4 latched permanently in the chamber into two- and three- tile assemblies (Fig. 4c,d). Designs 5 and 6 also latched together due to hydrodynamic pressure, however small latch travels and large fabrication biases (Fig 4b) caused these tiles to disassemble under shear force conditions.

The ability of microtiles with latch design 4 to assemble

under achievable flow conditions within a microfluidic chamber makes it a good candidate for further work in DFA experiments. Furthermore, based on the latching forces calculated in Table 1, we can conclude that the maximum hydrodynamic forces applied to the tiles under normal flow conditions are on the order of 800 μN. Future work will compare this number to those calculated using computational fluid dynamics software simulations of the same system.

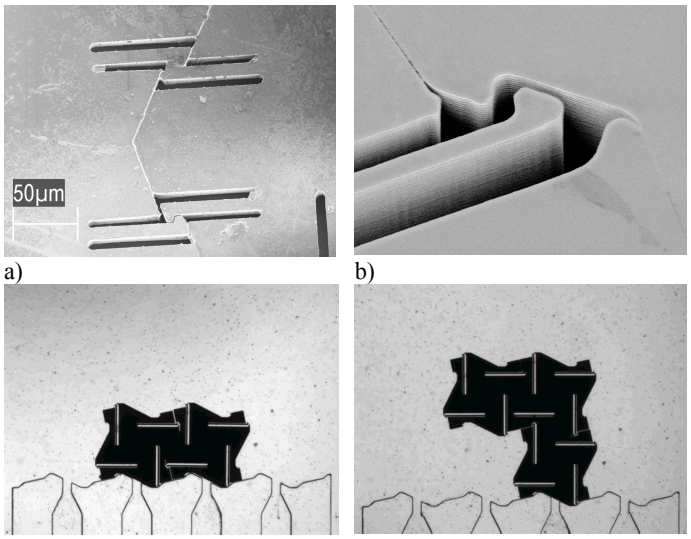


Figure 4: Latched Microtiles a) SEM of two manually-latched Design 1 tiles. b) SEM of latched Design 6 microtiles. A large fabrication bias causes poor mating. c), d) Frames from videos of the assembly of two and three Design 4 tiles (respectively).

3. ELECTRICAL INTERFACE

Design

The goal of the electrical interface design was to develop a method of establishing electrical contact between fluidically-assembled MEMS components at their edges. Such interfacing is important in extending our DFA concept to the assembly of MEMS devices. To date, electrical connections between fluidically-assembled components have only been established between their larger, horizontal surfaces using surface-energy minimization techniques.

In order to establish electrical connection between tiles, basic electrodes were patterned on the tiles connecting to contact pads on each tile side (Fig. 5). This design takes advantage of the well-defined mechanical interface in order to line up the electrical contacts and hold them together to form an electrical connection. Obviously tiles in this case would have to be assembled within a non-conducting fluid to prevent short-circuits. (Note that we have previously demonstrated assembly of silicon tiles in silicone oil [6]).

Fabrication

Electrodes were patterned Design 5 latching tiles etched through the device layer of an SOI wafer (but not released) as described above. We first deposited 15 μm of chromium (for adhesion), followed and 80 μm of gold using electron gun evaporation. For uniform metal deposition on the tile tops and sidewalls, the wafer was held at 45° to the evaporation material, and rotated in plane during deposition.

A thick layer (40 μm) of AZ-4903 photoresist was used to protect the electrode layer on the surface and sidewalls of tiles during a wet etch of the gold and chromium. The thick photoresist required a two-step expose/develop sequence. The first step included exposure and under-development of the desired electrode pattern on the top of the tiles, while the second step included a long exposure with a different mask of the thick layer of photoresist between the tiles (excluding the contact pads). A final develop then removed the remaining resist (Fig 5b). Tiles were released from the SOI wafer using a 49% HF oxide etch, which did not significantly damage electrode integrity.

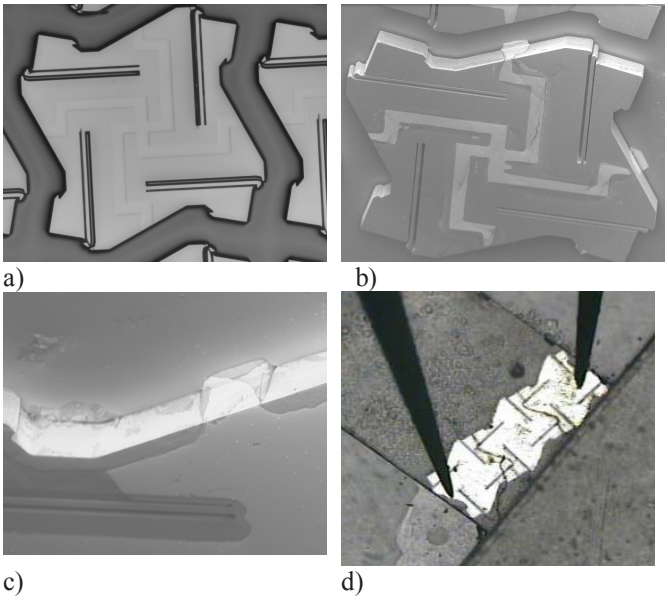
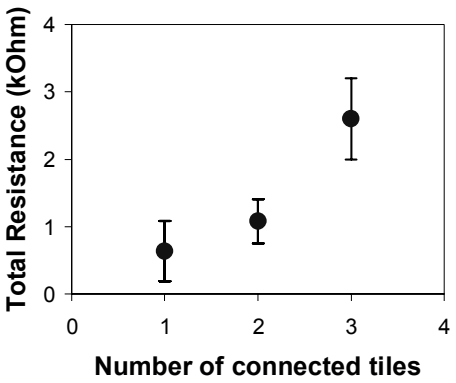


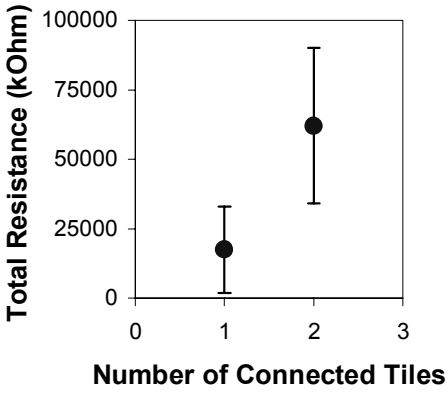
Fig. 5. Images of patterned microtiles. a) Optical Micrograph of resist coated tiles after first exposure step b) Scanning Electron Microscopy (SEM) image of patterned chromium/gold electrodes on top and sides of 500μm square by 30μm microtiles. c) SEM of contact pad electrode on tile sidewall allowing horizontal electrical connection between tiles. d) Measurement of resistance across three microtiles using contact probes.

Results

Fabrication yielded many tiles with intact electrodes and contact pads (Fig. 5a,c) although inconsistencies in photoresist coverage led to varying results. Electrical testing was completed to verify conductivity across tiles and between assembled microtiles (Fig. 5d). Resistance data was obtained using a multimeter probe station for one, two, and three-tile circuits (Fig. 6a). Tiles were manipulated and connected in silicone oil on a glass substrate using a pair of multimeter probe tips. As a control, the resistance across plain (electrodeless) silicon tiles was also measured (Fig. 6b).



a)



b)

Fig. 7. Resistance versus number of tiles for a) electrode-patterned and b) non-patterned silicon microtiles Data points represent average measured values. Error bars represent maximum and minimum measured values. These graphs show that conduction occurs through tiles connected in-plane through gold electrodes with resistance values on the order of 10^4x less than through silicon.

We used the resistance equation $R = \rho L / A$ to calculate the order of magnitude of the resistance R across the width of one silicon tile with gold and chromium electrodes on top. Using values of 2.4e-8, 13e-8, and 1.0e-3 Ω-m as the resistances of gold, chromium, and silicon at 20°C respectively, we calculated $R \approx 4.0\Omega$. Compared with the resistances measured across a single patterned tile (Fig. 7a), we conclude that R is negligible compared to contact resistance at the tile-probe and tile-tile interfaces. Under this assumption, using a least-squares regression, the average contact resistances between tiles and at the tile-probe interfaces were 880 Ω (0.00792 Ω·cm^2) and 280 Ω respectively.

5. CONCLUSIONS

We have presented the design and implementation of electrical and mechanical interfaces for fluidically-assembled planar MEMS components. We have demonstrated the ability of components with these interfaces to bond by way of passive mechanical latches and establish an electrical connection. This work forms an integral part of the development of a novel microassembly strategy which bridges the gap between bottom-up self-assembly and top-down direct-manipulation techniques. Future work in this direction could lead to MEMS devices capable of the on-demand self-assembly, repair, and reconfiguration that lead to the adaptability and robustness of biological systems.

ACKNOWLEDGEMENTS

This work has been funded in part by the US National Science Foundation program for Materials Processing and Manufacturing, Engineering Design, grant number 0634652. M. T. Tolley would also like to thank the Natural Sciences and Engineering Research Council of Canada for their support through the Postgraduate Scholarship program.

REFERENCES

[1] D. Philip, J. F. Stoddart, "Self-Assembly in Natural and Unnatural Systems", *Angewandte Chemie*, vol. 35, pp. 1154-1196, 1996.

[2] G. M. Whitesides, B. Grzybowski, "Self-Assembly At All Scales", *Science*, vol. 295, pp. 2418-2421, 2002.

[3] K. F. Böhringer, R. S. Fearing, K. Y. Goldberg, in *The Handbook of Industrial Robotics,* S. Nof, Ed., Wiley & Sons, New York, 1999, pp. 1045-1066.

[4] D. H. Gracias, J. Tien, T. L. Breen, C. Hsu, G. M. Whitesides, "Forming Electrical Networks in Three Dimensions by Self-Assembly", *Science*, vol. 289, pp. 1170-1172, 2000.

[5] U. Srinivasan, D. Liepmann, R. T. Howe, "Microstructure to Substrate Self-Assembly Using Capillary Forces", *J. MEMS*, vol. 10, pp. 17-24, 2001.

[6] M. Tolley, V. Zykov, D. Erickson, H. Lipson, *Proc. of Micro Total Analysis Systems (microTAS) 2006 Conference*, Tokyo, November 5-9 2006, pp. 1552-1554.

[7] M. A. Unger, H.-P. Chou, T. Thorsen, A. Scherer, S. R. Quake, "Monolithic Microfabricated Valves and Pumps by Multilayer Soft Lithography", *Science,* vol. 288, pp. 113-116, 2000.